

EU PVSEC PAPER

PV degradation curves: non-linearities and failure modes

Dirk C. Jordan*, Timothy J. Silverman, Bill Sekulic and Sarah R. Kurtz

National Renewable Energy Laboratory (NREL), 15013 Denver West Parkway, Golden, CO 80401, USA

ABSTRACT

Photovoltaic (PV) reliability and durability have seen increased interest in recent years. Historically, and as a preliminarily reasonable approximation, linear degradation rates have been used to quantify long-term module and system performance. The underlying assumption of linearity can be violated at the beginning of the life, as has been well documented, especially for thin-film technology. Additionally, non-linearities in the wear-out phase can have significant economic impact and appear to be linked to different failure modes. In addition, associating specific degradation and failure modes with specific time series behavior will aid in duplicating these degradation modes in accelerated tests and, eventually, in service life prediction. In this paper, we discuss different degradation modes and how some of these may cause approximately linear degradation within the measurement uncertainty (e.g., modules that were mainly affected by encapsulant discoloration) while other degradation modes lead to distinctly non-linear degradation (e.g., hot spots caused by cracked cells or solder bond failures and corrosion). The various behaviors are summarized with the goal of aiding in predictions of what may be seen in other systems. Published 2016. This article is a U.S. Government work and is in the public domain in the USA.

KEYWORDS

PV degradation; durability; reliability; failure mode; non-linearity

*Correspondence

Dirk C. Jordan, National Renewable Energy Laboratory (NREL), 15013 Denver West Parkway, Golden, CO 80401, USA.

E-mail: dirk.jordan@nrel.gov

Received 3 May 2016; Revised 31 August 2016; Accepted 7 September 2016

1. INTRODUCTION

Photovoltaic (PV) durability and reliability questions have attracted increased interest in recent years because of their technological and economic significance. Reliability is the ability to perform a required function for a given time interval and is often measured in terms of failure rate or as a probability for failure [1]. In contrast, durability relates to the time interval a system is performing its desired task and is in PV commonly measured as the degradation rate, the slow gradual loss of performance. Literature degradation rates were summarized and analyzed by some of the authors and were recently updated [2,3]. However, the fallacy lies in the word “rate” because of the intrinsic linearity assumption. While the linearity assumption may be a preliminarily appropriate choice, it is often violated in the infant or wear-out phase of a system’s life cycle. This can have significant economic consequences, as illustrated in Figure 1. Four different degradation curves, each of them observed (approximately) in field performance, are used in Monte Carlo simulation to quantify the effect on

levelized cost of energy (LCOE) [4]. The spider graphs of Figure 1(b) constitute the sensitivity analysis of the simulations. The most significant factors (for the ranges explored) on LCOE are the discount rate and initial cost indicated by the greatest range on the ordinate for each of the graph compartments. The curve characteristic of all the input variables does not change for the different input degradation curves. However, the mean of the graph shifts for the different degradation curves. The impact of the different degradation curves is ~ 1.1 c/kWh, making it the third most important factor after the discount rate and the initial cost. Therefore, measuring and including linear degradation rates in models may not be sufficiently accurate.

Besides the illustrated economic motivation, the technically compelling reason to determine degradation non-linearities is the development of lifetime prediction models. One pitfall of accelerated testing is that it may over-accelerate a specific failure mode while another failure mode may be masked that could turn out to be dominating in the field under potentially different use conditions [5]. To guard against this apparent danger, the

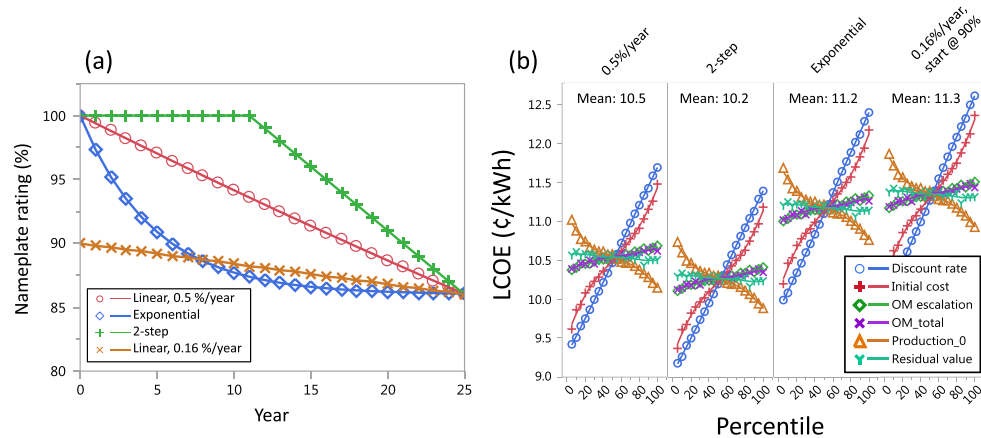


Figure 1. Monte Carlo simulation of various photovoltaic degradation curves' impact on levelized cost of energy (LCOE) after 25 years. Four different input degradation curves encountered in field measurements (a) and sensitivity analysis impact on LCOE (b). Discount rate is the rate at which future cash flows are discounted to present day values. Operational and maintenance (O&M) escalation takes into account increased O&M expenses with increasing age, and residual value is the value of the project after 25 years.

underlying failure mechanism, the physical and or chemical cause, must be understood. Therefore, understanding specific failure or degradation modes and their function with time is a crucial step in synchronizing accelerated tests and field test observations. Non-linearities are typically more easily observed in accelerated tests than in field observations because the faster changes are easier to detect. Perhaps because of the variety of conditions that modules are exposed to in field tests or because of the synergistic nature of some degradation modes, fielded modules often display a variety of degradation modes making it difficult to correlate a specific failure mode with a specific time series behavior.

In this paper, we aim to provide some examples of degradation modes and their different behavior as a function of time, although in some cases the exact function remains to be determined. We will start with the infant phase of a PV system's life cycle and then discuss examples in the wear-out phase.

2. METHOD AND OVERVIEW

Data were collected for a variety of modules and small systems deployed at the Outdoor Test Facility at the National Renewable Energy Laboratory in Golden,

Colorado. The data collection and analysis methodologies were described in References [6,7]. The soiling observed in this test field is typically 1–2%. In order to reduce the effects of the soiling on the degradation rate data, the irradiance sensors were cleaned only when the PV modules were also cleaned, typically by rainfall or at the time of I–V measurements.

A high-level summary of the results is shown in Table I. Although only one data set is shown for each line in the table, these observations are consistent with other observations either in the literature or in our own experience. Table I differentiates some of the changes seen immediately after deployment (infant phase) from those that may be seen after years in the field (wear-out phase). The one degradation mechanism we have seen to be mostly linear over the years is noted in the “Phase” column as “consistent” because we have observed this degradation to be constant over many years, although there is some evidence that after more than a decade the degradation rate may slow slightly.

3. INFANT PHASE

Many PV technologies, especially thin-film technologies, exhibit non-linearities at the beginning of their useful life.

Table I. Summary of degradation types, time scales and how they tend to appear for some technologies in specific phases.

Phase (direction)	Technology	Time scale	Degradation type
Infant (decrease)	a-Si	Months	LID, Staebler-Wronski
Infant (decrease)	CdTe	1–3 years	Metastability
Infant (decrease)	x-Si	Hours	LID, O-B complex
Infant (increase)	CIGS	Days, months	Metastability
Consistent	All	Years	Discoloration
Wear-out	All	Months, years	Series resistance
Wear-out	All	Months, years	Cracked cells, solder bond failure

a-Si, amorphous silicon; CdTe, cadmium telluride; x-Si, crystalline silicon; LID, light-induced degradation.

The initial rapid decline for amorphous silicon (a-Si) has been well documented [8]. The initial rapid decline occurs during several months before the onset of the long-term trend, as shown in Figure 2. Cadmium telluride (CdTe) — inverted blue triangles — may also pass through a transient regime that can range from 1 to 3 years before stabilization and normal performance commences [9,10]. Light-induced degradation can also affect crystalline silicon (x-Si) systems, particularly those fabricated with Czochralski-based wafers [11,12]. Yet, the time scale is typically much shorter than thin-film systems making it in generally difficult to detect in outdoor data. In contrast, some modern multi-crystalline cell designs may also lead to extended non-linearities in the infant phase [13]. The time series behavior can be modeled exponentially or separated into two distinct phases, the initial decline followed by a more stable phase. The former approach may be more accurate, yet the latter is often more convenient despite the subjectivity to determine the exact start of the more stable period. In contrast, the CIGS system shown here, which does not represent all CIGS technologies, shows a distinctly different behavior; an initial increase during the first several months of light exposure is followed by the onset of the long-term degradation. It is evident from these examples that the initial trend can be significantly different from the long-term behavior. In addition, if the initial phase is included in the evaluation, the long-term prediction would include a substantial, yet unintended bias. In this case, a sensible choice may be to exclude the initial phase that commences with light exposure to determine the ultimate long-term behavior. This choice may also be viable for known start-up issues such as incomplete connectivity of all strings in a system, for example.

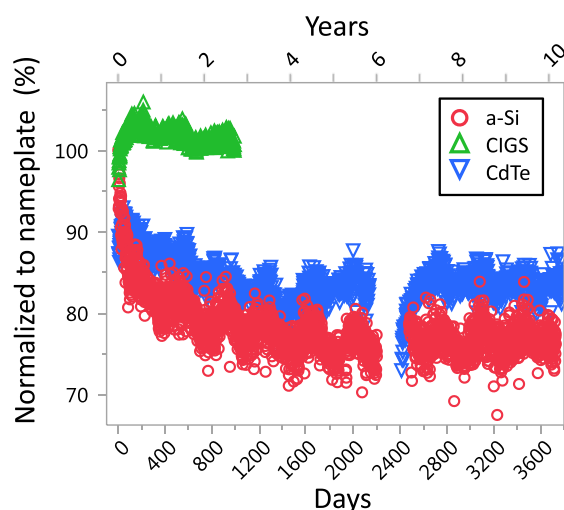


Figure 2. Initial non-linearities for thin-film technologies upon first light exposure. Nameplate ratings are often adjusted to align with the more stable performance.

4. WEAR-OUT PHASE

In the wear-out phase of a product, the failure rate increases as a function of time. The increasing number of failures may display a single mode or several; in addition, the failure modes may not be completely independent of each other. For example, delamination may initially only lead to extra current-dominated power loss because of the formation of an extra optical interface. As the delamination becomes more severe, the probability increases for moisture ingress. The moisture ingress may lead to internal circuitry corrosion and eventually even lead to internal circuitry failure. Each of these failure modes may exhibit a different power decline as a function of time, yet isolating these different functional forms is problematic. During the block buy program of the Jet Propulsion Laboratory in California, USA, the interdependency between different durability performance and failure modes was already recognized; however, the module design changed considerably in the subsequent decades [14]. Furthermore, observing non-linear trends in larger systems that may be dominated primarily by modules exhibiting approximately linear decline can be challenging even if the non-linear trend for a single module is fairly significant. More recently, the International Energy Agency PV Power Systems Program — Task 13 — published a detailed review of failures of PV modules based on literature and site visits [15]. The treatise discusses at length inspection tools, observed failures, and test methods. Different failure modes are classified by safety and their different time series behavior, for example, linear versus non-linear, although corroborating time series data were not provided. Several studies from different continents have emerged that investigated an ensemble of modules at different times of their life cycle [16–19]. Of these ensembles, the better performing modules and the central tendency of the modules appear to decline fairly linearly; however, the worst performing modules show non-linear behavior [3].

5. DISCOLORATION

The most commonly reported degradation mode is encapsulant discoloration, which may be aided by the fact that discoloration is also the most noticeable mode by visual inspection [20]. We refer to this as “degradation” rather than “failure,” as discoloration leads typically to lower performance but not necessarily to failure, even when considering soft failure limits such as a typical power warranty. Figure 3(a) shows a typical example of a linear degradation curve for a mono-crystalline (mono-Si) module that was fielded for 14 years. The module was installed at the National Renewable Energy Laboratory’s performance and energy rating testbed with current-voltage measurements taken every 15 min. The maximum power (P_{max}) decline of $(0.33 \pm 0.02)\%/year$ is dominated by short-circuit current (I_{sc}) decline $(0.31 \pm 0.01)\%/year$. The fill factor (FF) and the open circuit voltage (V_{oc})

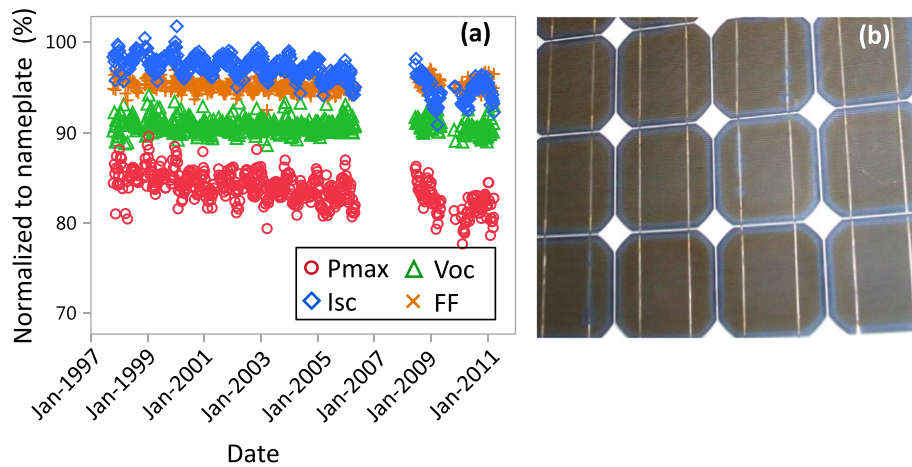


Figure 3. Mono-Si module I-V performance over 20 years of field exposure (a). The vertical axis shows the I-V parameter as a percentage of the nameplate rating. Discoloration in the center of the cells is shown (b) and some bleaching at the cell edges. Photo credit: Dirk Jordan, NREL PIX 36886.

display relative stability: $(0.01 \pm 0.01)\%/year$ and $(0.02 \pm 0.01)\%/year$, respectively, within the statistical uncertainty. The Pmax loss totals to less than 5% over the lifetime of the module; the transmission loss from the discoloration in the center of the cells is shown in Figure 3(b) with some bleaching at the cell edges corroborating the Isc dominated decline. The degradation appears to be approximately linear although a subtle non-linear trend that is masked by latent seasonality and measurement uncertainty cannot be completely excluded.

6. SOLDER BOND FATIGUE

In contrast, the x-Si module of Figure 4 that was exposed next to the module of Figure 3 shows initially a fairly stable behavior that appears to be followed by a concave decline. Pmax data were corrected to 45 °C module temperature, as it was a more typical value than 25 °C during the lifetime of the module at this particular location. Data acquisition problems led to ~1 year gap during which the module was exposed outside and continued to

degrade. A second interruption starting at month 71 was caused when the module was stored inside while the data collection system was upgraded. During this time, no additional degradation was observed; for clarity, this section was removed from Figure 4. It is interesting to note that a power fit provides a better fit to the data than a linear fit. The I-V characteristics that are taken at the beginning and almost exactly after 10 years display clear signs of series resistance increase. Series resistance increase has been associated with thermal mechanical fatigue of solder joints, solder corrosion or ribbon fatigue [15,21–23].

This module exhibited many cracks in the cell and string interconnect ribbons, an example of which is shown in Figure 5(a). The cracks appear to have not caused a complete failure; however, they affirm the increased series resistance and the hot spots in the infrared image that occur along the cell interconnect ribbons (Figure 5(b)). The interconnect connections could be improved by applying pressure to the front side of the module. The electroluminescence images of Figure 6 demonstrate the change in connection pointed out by the arrows.

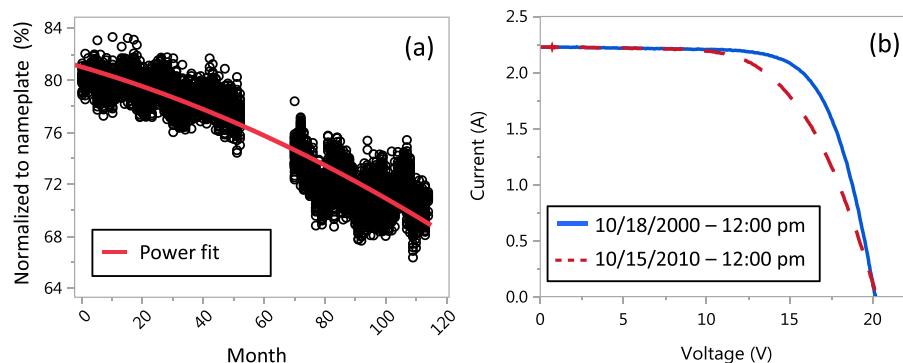


Figure 4. Time series behavior for series resistance impacted x-Si module over 10 years (a). Initial and end-of-life I-V shows clear signs of series resistance increase (b).

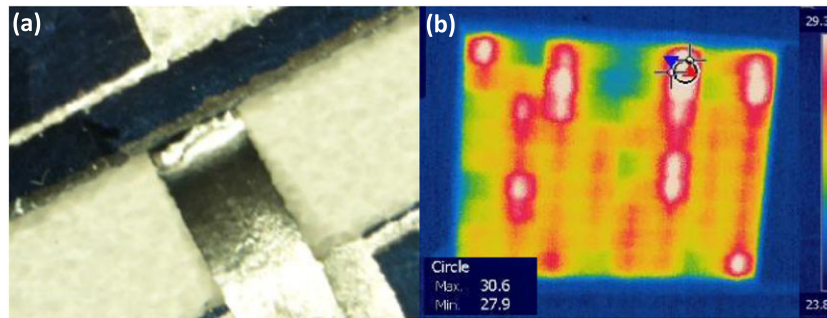


Figure 5. Visual image of one of the cracks in the cell interconnect ribbon (a). Infrared image showing hot spots along interconnect ribbons (b). Photo credit: Dirk Jordan, NREL PIX 38042 and 38044.

7. SOLDER BOND FAILURE

Hot spots are important because of safety considerations. In side-by-side comparisons, modules affected by hot spots displayed greater power loss compared with unaffected modules [19,24,25]. Hot spots as a failure mode can have different causes, such as solder bond failures or cracked cells, as we will discuss in this section.

Thermal cycling can eventually lead to solder bond failures. Figure 7(a) shows I-V parameters of a single string over nearly 22 years of field exposure that was recently affected by a hot spot. The hot spot was caused by solder-bond failure between the ribbon and the cell busbar. A characteristic burn mark was observable on the front and the backsheet of the module (b). The hot spot was first detected in 2014 but the temperature was measured to be in the 50–60 °C range. After an additional 1½ years of field exposure, the hot spot had significantly increased in temperature to 110–130 °C. I-V parameter analysis of the affected string shows a fairly linear decline during 20 years that was correlated equally to FF and I_{sc} losses. However, the more recent evaluation concluded that the power loss is now following a different path that is more significantly correlated to FF loss.

8. CRACKS

Cracked cells can be another mechanism for hot spots, as illustrated in this section in a mono-Si module after more than 10 years of field exposure. The I-V parameters for this

particular module are presented in Figure 8(a), which were measured by four different methods. Initially, a drop of several percent can be seen that appears to be dominated by current loss and could be associated with light-induced degradation. For the subsequent 5 years, very little change in all parameters can be discerned until the appearance of the crack-induced hot spot. The degradation slope changes and the power loss becomes FF-dominated. More frequent data points are needed to ascertain the exact functional form, as it could follow a two-step or possibly a more gradual power decline. The overlay from the large area continuous solar simulator (LACSS) shows the increased series resistance in the module, Figure 8(b).

The infrared image indicates a moderate hot spot (ca. 60 °C), Figure 9; electroluminescence image, not shown here, exhibited cracks in several cells, but only the crack in one cell resulted in a hot spot. The loss in power is related to the loss of current flow and is a complex function of the direction of the cracks as well as the integrity of the metallization (grid lines and busbars). It appears that some cracks have a more deleterious impact on the module power performance than others [26].

More frequent data are necessary; however, the best analytical practices are also required to accurately determine the functional form and ascribe them to specific failure modes, as is illustrated in the next example.

I-V parameters that were taken quarterly (a) and continuous data (b) for a Shell E80 CIS system are shown in Figure 10 [27]. The measurements were made without washing the system and therefore display some noise.

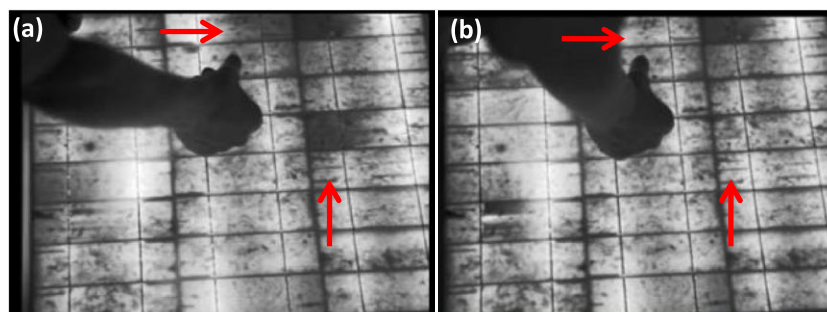


Figure 6. Electroluminescence images before (a) and while applying (b) pressure to the front side. The arrows point out changes in the luminescence because of improved conductivity through bridging of the gaps. Photo credit: Tim Silverman, NREL PIX 38045 and 38046.

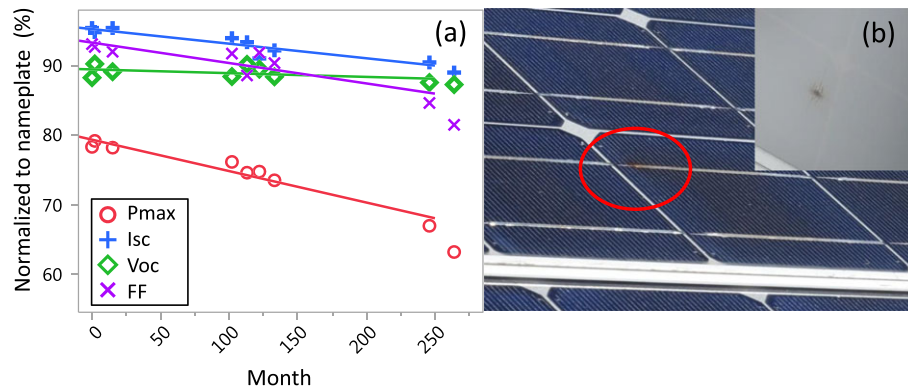


Figure 7. Solder bond failure-induced hot spot and its time series effect (a) and visual front and back-side images (b). This particular module was part of a 20-year-old system. The I-V traces may show increased degradation. Photo credit: Dirk Jordan, NREL PIX 36887.

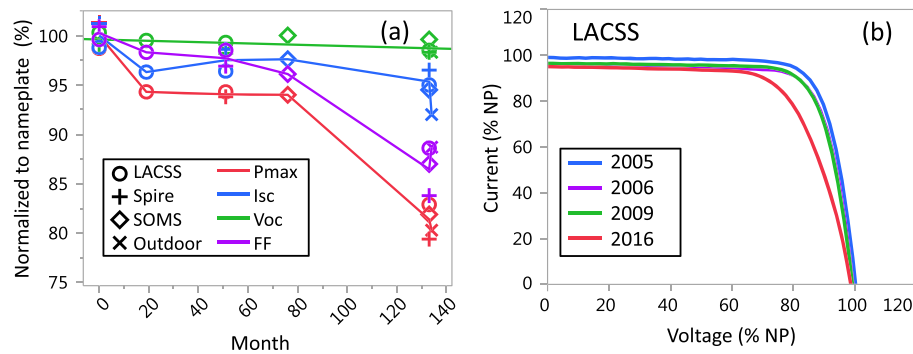


Figure 8. I-V parameters of the hot-spot module for more than 10 years exposure, as measured by four different methods (a). Large area solar simulator measurements (b) show series resistance increase.



Figure 9. Infrared image of a mono-Si module that has been fielded for more than 10 years with a hot spot caused by a cell crack. Photo credit Dirk Jordan, NREL PIX 36888.

Despite this noise in the data, the curve for Pmax appears to consist of two distinct sections. In the first 6 years, the system appears without any significant degradation. In the 6th to 7th year, a downward trend begins to emerge that is mostly caused by FF losses. During that period, visible

cracks in three modules were observed from the front (Figure 11). Isc and Voc appear to be stable over the entire 10 years field exposure.

The temperature-corrected array responsivity (blue circles) shows the two distinct degradation sections clearly;

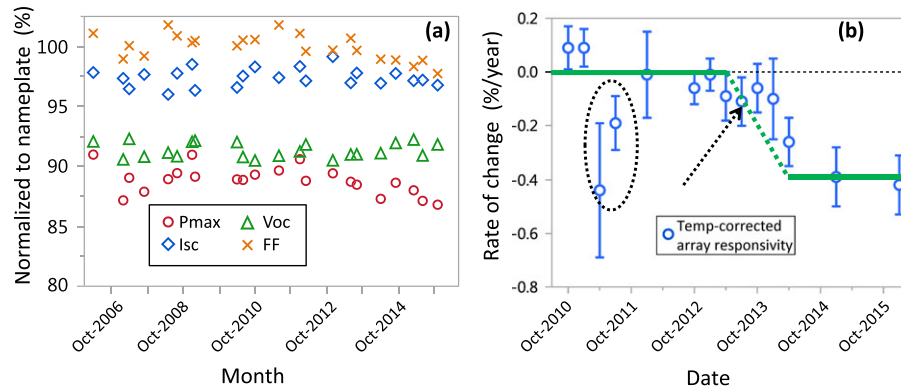


Figure 10. Outdoor measured I-V parameters for a Shell CIS system for a 10-year period (a). Continuous data for the system analyzed the temperature-corrected array responsivity (blue circles). The dashed oval indicates the time period of a drifting current transducer and the dashed arrow identifies when cracks first were observed.

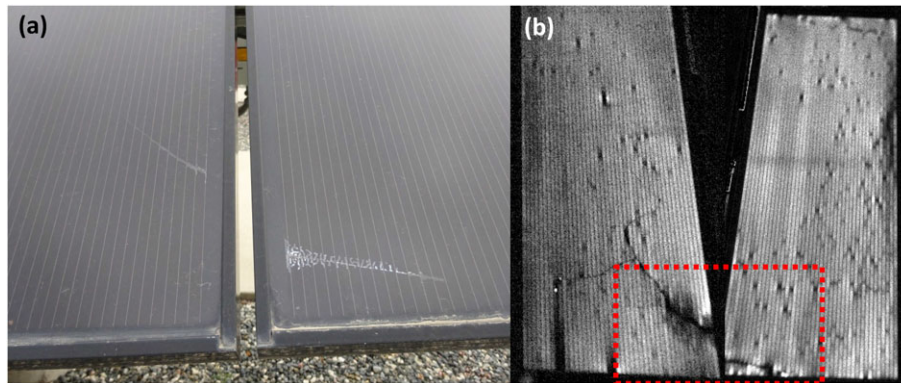


Figure 11. Two modules of a Shell E80 CIGS system after 10 years of field exposure. Visual image (a) is close up of the photoluminescence image (b) indicated by a red dashed rectangle. Photo credit Tim Silverman, NREL PIX 36890.

this technique provides reduced uncertainty relative to the more commonly used performance ratio [7]. Furthermore, a third section becomes clear with the temperature-corrected array responsivity that is indicated by a dashed oval. This time preceded our implementation of daily, automated data quality checks and was caused by a drifting current transducer. It was not reflective of the system performance but indicated data collection problems. After replacement of the transducer, the system returned to near zero degradation before the cracking of the modules. At first, the severity of the decline is surprising, as the cracks appear not very severe, yet the cracks are not located in the front glass but the active cell area. Photoluminescence corroborates the significant decline dominated by FF losses, as the cracks extended far more into the module than is visible to the naked eye.

It is conceivable that more two-step profile curves will become observable in the future, not as a result of different underlying degradation mechanisms but as a result of system design choices. Systems with high DC-to-AC ratios, as it is becoming more common, may exhibit a two-step profile regardless of the functional form of the underlying

degradation mechanism. As module prices have fallen, the balance-of-system components have become a larger percentage of the overall project cost. As a result, project costs can be reduced if the inverter is undersized, limiting the input to the inverter's capability during the highest producing periods of the year. The effect of this so-called inverter clipping is that such a system may not exhibit easily detectable degradation until many years of field exposure depending on used metrics and analytical methods.

9. CONCLUSION

Degradation rates are important for financial projections and may be indicative of different degradation modes. However, as modeling of PV performance becomes more sophisticated, degradation rates based on the assumption of linearity may not be sufficiently accurate. Non-linear trends at the beginning of life or during the wear-out phase are important to detect and understand economically and technically. Monte Carlo simulation of LCOE showed the significant effect of the shapes of degradation curves.

Technically, accurately identifying non-linearities in degradation paths is essential for service lifetime predictions. The most commonly reported degradation mode, encapsulant discoloration, appears to be associated with an approximately linear decline that is correlated to I_{sc} losses. However, a subtle non-linear decline that may be difficult to detect over common variations in outdoor measurements cannot be excluded. In contrast, series resistance increases caused by thermal mechanical solder bond fatigue appears to follow a delayed concave degradation trajectory. Cracked cells or complete solder bond failure show a more significant decline after the failure occurrence. In general, more frequent acquisition of data needs to be coupled with optimized analytical methods to delineate subtle trends that are often masked by measurement noise.

ACKNOWLEDGEMENTS

We would like to thank Jose Rodriguez for measurements and maintenance of the systems and NREL's measurement group. This work was supported by the U.S. Department of Energy under Contract No. DE-AC36-08-GO28308 with the National Renewable Energy Laboratory.

REFERENCES

1. International Electrotechnical Commission 60050-191, Dependability and quality of service, 1990.
2. Jordan DC, Kurtz SR. PV degradation rates – an analytical review. *Progress in Photovoltaics Research and Application* 2013; **21**(1): 12–29.
3. Jordan DC, Kurtz SR, VanSant KT, Newmiller J. Compendium of photovoltaic degradation rates. *Progress in Photovoltaics Research and Application* 2016; **24**(7): 978–989.
4. Short W, Packey DJ, Holt T, A manual for the economic evaluation of energy efficiency and renewable energy technologies, Report NREL/TP-462-5173, March 1995.
5. Meeker WQ, Escobar LA. Pitfalls of accelerated testing. *IEEE Transaction on Reliability* 1998; **47**(2): 114–118.
6. del Cueto JA. Review of the field performance of one cadmium telluride module. *Progress in Photovoltaics Research and Application* 1998; **6**: 433–446.
7. Jordan DC, Kurtz SR. The dark horse of evaluating long-term field performance—data filtering. *IEEE Journal of Photovoltaics* 2014; **4**: 317–323.
8. Staebler DL, Wronski CR. Optically induced conductivity changes in discharge-produced hydrogenated amorphous silicon. *Journal of Applied Physics* 1980; **51**(6): 3262–3268.
9. Ngan L, Strevel N, Passow K, Panchula AF, Jordan D, Performance characterization of cadmium telluride modules validated by utility-scale and test systems, *Proceedings of the 40th IEEE Photovoltaic Specialists Conference*, Denver, CO, USA, 2014, 1957–1962.
10. Strevel N, Trippel L, Gloeckler M. *Performance Characterization and Superior Energy Yield of First Solar PV Power Plants in High-Temperature Conditions*. Photovoltaics International, 2012.
11. Broek KM, Bennett IJ, Jansen MJ, van der Borg NJC, Eerenstein W, Light and current induced degradation in p-type multi-crystalline cells and development of an inspection method and a stabilisation method, *Proceedings of the 27th European Photovoltaic Solar Energy Conference and Exhibition*, Frankfurt, Germany, 2012, 3167–3171.
12. B Sopori, P Basnyat, S Devayajanam, S Shet, Y Mehta, J Binns, and J Appel, “Understanding light-induced degradation of c-Si solar cells,” *Proceedings of the 38th IEEE Photovoltaic Specialists Conference*, Austin, TX, USA, 2012, 1115–1120.
13. Fertig F, Kersten F, Petter K, Bartsch M, Stenzel F, Mette A, Klöter B, Müller JW. *Light and Elevated Temperature Induced Degradation of Multicrystalline Silicon Solar Cells and Modules*. Workshop on Crystalline Silicon Solar Cells & Modules: Materials and Process: Vail, CO, USA, 2016.
14. Ross Jr. RG. Reliability and performance experience with flat-plate photovoltaic modules. *Proceedings of the 4th European Photovoltaic Solar Energy Conference*, Stresa, Italy, 1982; 169–179.
15. Köntges M, Kurtz S, Packard C, Jahn U, Berger KA, Kato K, Friesen T, Liu H, Van Iseghem M, Performance and reliability of photovoltaic systems, Subtask 3.2: Review of Failures of Photovoltaic Modules, International Energy Agency, Report IEA-PVPS T13-01:2014, 2014.
16. Jordan DC, Sekulic B, Marion B, Kurtz SR. Performance and aging of a 20-year-old silicon PV system. *Journal of Photovoltaics* 2015; **5**(3): 744–751. DOI:10.1109/JPHOTOV.2015.2396360
17. Chamberlin CE, Rocheleau MA, Marshall MW, Reis AM, Coleman NT, Lehman PA, Comparison of PV module performance before and after 11 and 20 years of field exposure, *Proceedings of the 37th IEEE Photovoltaic Specialists Conference*, Seattle, WA USA, 2011, 101–105.
18. L Abenante, F De Lia, S Castello, Long-term performance degradation of c-Si photovoltaic modules and strings, *Proceedings of the 25th European Photovoltaic Solar Energy Conference*, Valencia, Spain, 2010, 4023–4026.

19. Friesen T, Chianese D, Realini A, Friesen G, Burà E, Virtuani A, Strepparava D, Meoli R, TISO 10 kW: 30 years experience with a PV plant, *Proceedings of the 27th European Photovoltaic Solar Energy Conference*, Frankfurt, Germany, 2012, 3125–3131.
20. Jordan DC, Kurtz SR. *Field experience: Degradation Rates, Lifetimes & Failures*. PV Module Reliability Workshop: Lakewood, CO, USA, 2016.
21. Quintana MA, King, DL, 2002. Commonly observed degradation in field-aged photovoltaic modules, *Proceedings of the 29th IEEE Photovoltaic Specialists Conference*, New Orleans, USA, 1436–1439.
22. Bosco N, Silverman TJ, Wohlgemuth J, Kurtz S, Inoue M, Sakurai K, Shioda T, Zenkoh H, Hirota K, Miyashita M, Tadanori T, Suzuki S, Evaluation of Dynamic Mechanical Loading as an Accelerated Test Method for Ribbon Fatigue, *Proceedings of 29th European Photovoltaic Solar Energy Conference*, Amsterdam, Netherlands, 2014. 2484–2489.
23. Dubey R, Chattopadhyay S, Kuthanazhi V, John J, Arora BM, Kottantharayil A, Narasimhan KL, Solanki CS, Kuber V, Vasi J, Kumar A, Sastry OS. *All-India Survey of PV Module Degradation: 2013*. National Centre for Photovoltaic, Research and Education Indian Institute of Technology Bombay National Institute of Solar Energy: Mumbai, India, 2013.
24. Bradley A, Hamzavy B, Gambogi W. Analysis of the degradation and aging of a commercial photovoltaic installation. *Proceedings of the SPIE* 2014; **9179**. DOI:10.1117/12.2062046
25. Chattopadhyay S, Dubey R, Kuthanazhi V, John JJ, Vasi J, Kottantharayil A, Arora BM, Narsimhan KL, Solanki CS, Bora B, Singh YK, Sastry OS. *Effect of Hot Cells on Power Degradation Rate of PV Modules*. PV Module Reliability Workshop: Lakewood, CO, USA, 2016.
26. M Köntges, S Kajari-Schröder, I Kunze, U Jahn, Crack statistic of crystalline silicon photovoltaic modules, *Proceedings of the 26th European Conference on Photovoltaic Solar Energy*, Hamburg, Germany, 2011, 3290–3294.
27. Jordan DC, Kurtz SR, Thin-film reliability trends toward improved stability, *Proceedings of the 37th IEEE Photovoltaic Specialists Conference*, Seattle, WA, USA, 2011, 827–832.